Amphiphilic platelets at a liquid interface

David H. Boal and Mark Blair*
Department of Physics, Simon Fraser University, Burnaby, British Columbia, Canada V5A 1S6
(Received 27 September 1990)

A model is presented for the behavior of amphiphilic platelets at an interface between immiscible liquids. In the model Hamiltonian, the edges and faces of a cylindrical platelet have different strengths of interaction with a given liquid. For almost all of their parameter space, the model platelets prefer to sit at the interface rather than in either liquid. However, the ground-state orientation of the platelets (flat or upright) is found to be a function of cylinder geometry and strengths of interaction. The equation of state of a platelet system is investigated using a simplified version of the model. At low temperatures, there is a rapid change in platelet orientation with pressure, but this does not appear to be a phase transition. At high pressure, the platelet system takes on the appearance of a nematic phase.

I. INTRODUCTION

The technique of exfoliation[1–3] has been used to make several novel materials in which the fundamental building block is a thin sheet that is a monolayer thick and around 1000 Å across. A common chemical composition of many monolayers studied so far is MX_2, where M=Nb, Ta, Mo, or W and X=S or Se. The sheets have a rigid in-plane geometry, but may be flexible out-of-plane. Of interest in this paper is the observation that the monolayers may collect at the interface between immiscible liquids, an example being the interface between a polar liquid like water and a nonpolar liquid like an organic solvent.

It has been suggested[4–6] that the attraction of the monolayer to the interface arises because the basal plane forming the "face" of the monolayer is attracted to the organic liquid, while the edge of the sheet is attracted to the polar liquid. Here, we investigate this possibility quantitatively by constructing a model of amphiphilic cylinders which is applicable to geometries from disks to rods. In the model Hamiltonian described in Sec. II, the faces and edge of the cylinder have different strengths of attraction to different fluids (the edge being more attracted to one liquid while both faces are more attracted to the other liquid). In Sec. III, the ground states of this amphiphilic cylinder are shown to lie at a liquid-liquid interface over almost all of the model's parameter space, with the cylinder's orientation at the interface depending on differential attraction, surface tension, and cylinder geometry. This behavior shares features found[7] for model polymers with random attraction (along the chain) to two fluids.

As well as the ground states of these amphiphilic cylinders, we investigate the properties of a system of such objects at finite temperature and pressure. Unfortunately, there is a rather large parameter space involved in the model, and so in Sec. IV we develop a restricted orientation model in which the cylinder is allowed to lie with its axis of revolution either perpendicular or parallel to the interface (for a disk, we refer to these orientations as flat or upright, respectively). These two orientations are, in fact, either ground states or metastable states over much of the general model parameter space, so the simplified model contains similar physics to that expected for the general model.

In Sec. V we investigate the behavior of an N-P-T ensemble in the restricted orientation model. The equation of state, obtained computationally, shows the expected ideal-gas-like behavior at high temperature, and a more abrupt flat-to-upright transition as a function of pressure at low temperature. At high pressure, the upright platelets become ordered, similar to the nematic phases observed[8–11] in hard spherocylinders, etc. Our conclusions are summarized in Sec. VI.

In all of our calculations, the platelets interact with each other only through a hard-core repulsive potential that prevents overlap. We have omitted other interactions simply to reduce the parameter space. In further work, attractive interactions between the cylinders will be added to allow exploration of other aspects of interfacial behavior, as has been done in liquid-crystal studies.[12]

II. MODEL HAMILTONIAN

In Refs. 4 and 5 it is proposed that the reason why MoS_2 sheets are attracted to water–organic liquid interfaces lies in the differential attraction of the basal plane and edge of the MoS_2 monolayer to the liquids. In particular, it is suggested that the basal plane is attracted to the organic liquid while the edges are polar and are attracted to water. There are many ways in which such an interaction can be modeled. A particularly simple form that we propose in this paper is to represent the monolayer as a cylindrical platelet of radius R and thickness T. Although we use the word "platelet," in fact all cylindrical geometries between disks and rods are included in the parameter space we investigate.

The center of the platelet lies a distance z above the two-liquid interface, where liquid 1 lies atop liquid 2 and

the interface is assumed to be flat. The normal to the plane of the platelet makes an angle α with respect to the normal to the interface. Because the two faces of the model platelet are equivalent, the full range of orientations can be found for $0 \leq \alpha \leq \pi/2$. We define positive values of z to lie in liquid 1. For the time being, we do not reduce the number of parameters by quoting the thickness in terms of the radius, etc.

The interface may intersect the platelet in a number of ways, depending on its position and orientation parameters z and α. The possibilities are illustrated in Fig. 1 for $z > 0$. We use labels I, II, and III to distinguish whether there are 0, 1, or 2 intersections of the interface with the cylinder's faces, respectively. Defining the quantities

$$D = R\,[1+(T/2R)^2]^{1/2} \tag{1}$$

and

$$\sin\delta = T/2D\ , \tag{2}$$

the boundary regions on Fig. 1 follow from simple geometry. The solvent interface does not intersect the platelet at all if

$$z > R\left[\sin\alpha + \frac{T}{2R}\cos\alpha\right]\ . \tag{3}$$

The boundary between regions I and II is given by

$$z_{\mathrm{I,II}} = D\sin(\delta-\alpha) \tag{4}$$

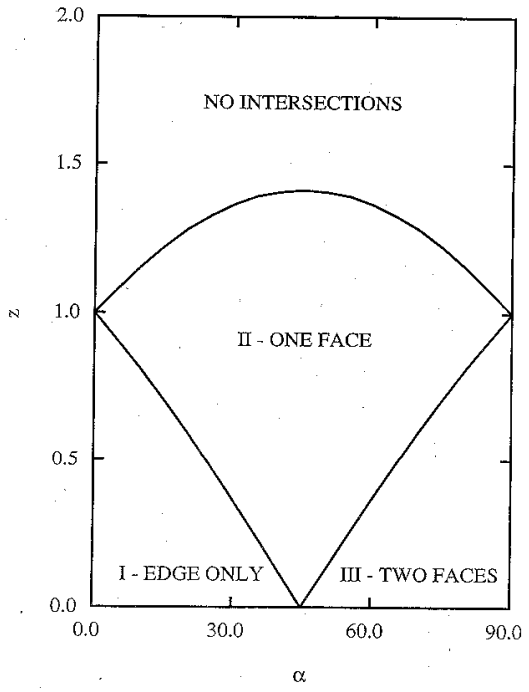

FIG. 1. Platelet orientations with respect to the interface. The labels I, II, and III correspond to situations in which the interface intersects the cylinder and there are 0, 1, or 2 intersections of the interface with the faces of the platelet, respectively. The boundaries are drawn for $T/2R = 1$.

while that between regions II and III is

$$z_{\mathrm{II,III}} = D\sin(\alpha-\delta)\ . \tag{5}$$

We propose the following model Hamiltonian to represent the interaction between the platelet and the liquids:

$$H(z,\alpha) = -k_{F1}A_{F1} - k_{E1}A_{E1} - k_{F2}A_{F2} - k_{E2}A_{E2} - s_{12}A_{12}\ . \tag{6}$$

In this expression, the areas A_{Fi} and A_{Ei} are the areas of the face and edge of the platelet exposed to liquid i. The area between the liquids which the platelet displaces when it is at the interface is A_{12}. The constants k represents the strength of the interaction between the liquids and the face or edge of the platelet, while s_{12} is the surface tension between the liquids. Positive values for k represent attraction, while positive s indicates that removal of liquid-liquid interfacial area lowers the energy. Analytical expressions for the areas in Eq. (6) as a function of z and α are not difficult to obtain and are summarized in the Appendix.

III. GROUND-STATE ORIENTATIONS

As a first application of the model Hamiltonian, we examine the ground-state orientations of the platelets. Since we are interested in the minimum of $H(z,\alpha)$ as a function of z,α it is convenient to eliminate the areas exposed to liquid 1 in favor of those exposed to liquid 2 and the total areas A_{FT} and A_{ET} of the two faces and edge, respectively. The Hamiltonian is then rewritten as

$$H(z,\alpha) = g_F A_{F2} - g_E A_{E2} - s_{12}A_{12} - (k_{F1}A_{FT} + k_{E1}A_{ET})\ , \tag{7}$$

where

$$g_F = k_{F1} - k_{F2}\ , \tag{8a}$$

$$g_E = k_{E2} - k_{E1}\ . \tag{8b}$$

The term in parentheses in Eq. (7) is just the energy of a platelet completely surrounded by liquid 1, an energy which we will define as $E_1 = -(k_{F1}A_{FT} + k_{E1}A_{ET})$. Since we are interested in the platelet position with respect to the interface at zero temperature, then E_1 makes a convenient reference point against which to compare energies. Experimentally, liquid 1 is often organic, while liquid 2 is polar like water. In the systems investigated experimentally, the edge appears to be more strongly attracted to liquid 2, while the face appears to be more strongly attracted to liquid 1. Hence, Eqs. (8) are arranged so that g_F and g_E are positive for this situation in order to facilitate comparison with experiment.

First, we consider the situation in which the surface tension s_{12} vanishes. The energy minima of a variety of platelet orientations are summarized in Fig. 2. It is convenient to define two dimensionless quantities related to the energy and geometry of the platelet,

$$\Delta\varepsilon = \frac{H(z,\alpha) - E_1}{\pi R^2 g_F} \tag{9a}$$

and

$$\eta = \frac{g_E T}{g_F R} . \tag{9b}$$

Since E_1 has been subtracted from $H(z,\alpha)$ in the figure, $\Delta\varepsilon$ of the platelet solely in liquid 1 is always zero. The energy of the platelet solely in liquid 2 is higher (lower) than E_1 if $\eta < 1$ ($\eta > 1$).

The two other curves in the figure are the minimum energies of the platelet at the interface for the extreme values of $\alpha = 0$ and $\alpha = \pi/2$. The $\alpha = 0$ curve is linear as a function of $g_E T/g_F R$. For small values of η, it is energetically more favorable for the platelet to be in liquid 1 than to lie flat at the interface, where half of its facial area is exposed to liquid 2. The $\alpha = 0$ interfacial configuration is not energetically favored over pure liquid 1 unless $\eta > \frac{1}{2}$. However, $\alpha = 0$ is not always the lowest-energy orientation at the interface. The energy of the platelet sitting "upright" at the interface is nonlinear and depends on the relative values of A_{F2} and A_{E2} through trigonometric functions. The minimum energy value for $\alpha = \pi/2$ is shown by the curve which ends at $\eta = 2$. For $\eta < 0.56$, there is an $\alpha = \pi/2$ configuration which lies below the $\alpha = 0$ minimum energy configuration. Above this value of η, there is always an $\alpha = 0$ configuration with lower energy than the $\alpha = \pi/2$ minimum energy configuration.

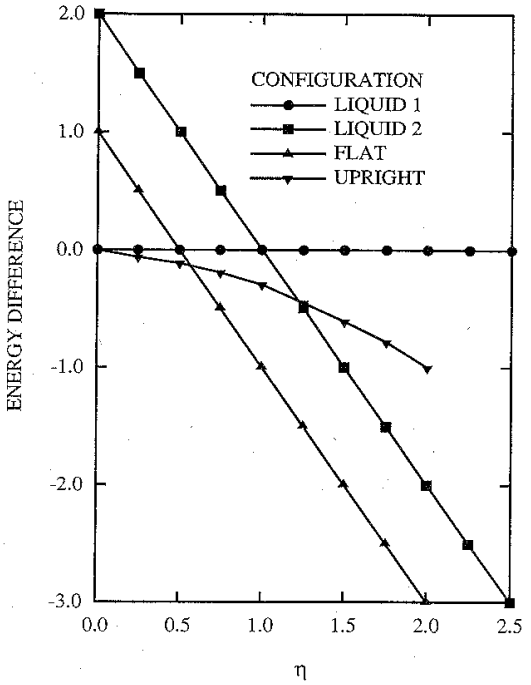

FIG. 2. Energy minima of a single platelet at the interface (in either a flat or upright position) or completely surrounded by a single liquid for the case of zero surface tension. The quantity $\eta = g_E T/g_F R$, and the energy difference is $\Delta\varepsilon$ as defined in Eq. (9a).

What the figure shows is that at no value of $g_E T/g_F R$ is it energetically more favorable for the platelet to sit isolated in one liquid: unless $\eta = 0$, there is *always* an energetically more favorable configuration at the interface. Further, there is only a small range in parameter space at which the platelet does *not* lie flat at the interface. These "upright" configurations occur for relatively weak attraction of the edge to liquid 2, because either the interaction strength is weak or the platelet is thin. It is also interesting to note that $\alpha = \pi/2$ orientation may be a metastable state when $\alpha = 0$ is the ground state. This is true for the $\alpha = \pi/2$ configurations for the range $0.56 < \eta < 2$. For $\eta > 2$, the $\alpha = \pi/2$ configuration is no longer metastable in that there is no energy barrier against decay to the ground state.

All of the above discussion assumes zero surface tension. If the surface tension between the liquids is nonzero, then the attraction of the platelet to the interface is even stronger. The crossover point between $\alpha = 0$ and $\alpha = \pi/2$ minimum energy configurations depends on s_{12}, although it may be the case that neither of these extremes is the ground state in the presence of surface tension. For example, if $g_F = g_E = 0$, then the ground state is that of maximum A_{12}, in which the interface runs diagonally through the platelet. Hence, we conclude that the platelets are always attracted to the interface for our model Hamiltonian with positive values for the energy coefficients.

IV. A SIMPLIFIED MODEL FOR THERMODYNAMIC STUDIES

Suppose now we consider not the energetics of a single platelet, but rather the behavior of many platelets near the interface at finite temperature and pressure. Such a system may have many properties: there may be transitions from flat to upright phases as a function of pressure and the upright phase may behave like a nematic liquid crystal. Unfortunately, calculating the thermodynamics of an ensemble of model platelets is an exhaustive task because of the large parameter space involved. A more computationally tractable model can be developed for thermodynamic studies if we restrict our interest to whether the platelets lie flat or upright at the interface as a function of pressure and temperature. The simplifications and calculational techniques are given in this section, and results are presented in Sec. V.

Let us assume that the only values available to the orientational angle α are 0 and $\pi/2$. Further, let us assume that the platelet is very thin ($T \to 0$) and that the platelet's center is restricted to lie at the interface ($z = 0$). The energy difference between the flat and upright orientation is then taken to be a constant, E_0. Now, an interesting situation arises if $E_0 > 0$ where a flat platelet has a lower energy than an upright one. Since the flat platelet also has less translational freedom in an ensemble, there is a competition between energy and entropy which may lead to a sharp transition between flat and upright phases.

We use the traditional Metropolis Monte Carlo tech-

nique[13] to investigate the thermodynamics of the restricted orientation model. A total of N platelets are placed in a two-dimensional square box of length L. The box has periodic boundary conditions and a variable size whose average value is a function of the pressure on the system. As throughout this paper, we neglect interactions between the platelets except for their geometrical hard-core repulsion required to prevent them from overlapping. The internal energy of the system is just the sum of the individual platelet energies, including the "step-function potential" representing the hard-core repulsion between platelets. Trial positional moves are made on each platelet in turn by shifting the platelet's position randomly within a square of length $2s$ to the side, centered on the platelet's current position. The move is rejected if the platelet intersects another. At the same time as the trial positional move is made, the orientation angle α of each platelet is randomly set to 0 or $\pi/2$. This change is conditionally accepted with the usual Boltzmann weight according to $\exp(-\Delta\varepsilon_0)$ where $|\Delta\varepsilon_0|=\beta E_0$ and $\beta=1/k_BT$. For $s=0.1$ (in platelet radii) we find that typically 35–50 % of the trial positional moves are accepted for much of the energy and pressure parameter space examined.

Finally, at the end of each sweep over the N platelets, an attempt is made to rescale the system length scale. The rescaling consists of changing all coordinates x to $x'=(1+\omega)x$, where ω is a number distributed randomly on the interval ± 0.02 and where the center of the confining box sits at the origin. The rescaled system is checked for platelet overlap if ω is negative. The trial configuration is conditionally accepted according to the pseudo-Boltzmann factor

$$W=\exp[-\beta P\Delta A+N\ \ln(1+\Delta A/A)]\ , \tag{10}$$

where ΔA is equal to the trial area $(L')^2$ less the "old" area L^2. The acceptance rate for the rescaling varies from 5% to 15% for most system sizes investigated.

The Monte Carlo method produces successive configurations at the end of each sweep which are highly correlated. Hence, we sample configurations which are separated by 50 000 sweeps over the N platelets. Fifty such configurations are used in determining the expectations presented in the next section. At the highest pressures and lowest temperature considered the system is allowed to relax for 500 000 sweeps before configuration sampling begins. The initial state for all systems is a low-density system with the platelets randomly distributed in position and orientation in a box with $L>(4N)^{1/2}$.

V. EQUATION OF STATE

We concentrate our computational efforts on a system of 128 platelets. In two dimensions, such a system is large enough to obtain statistically accurate values for almost all of the observables reported. A total of four temperatures are investigated ($\beta E_0=2$, 4, 6, and 8) and ten pressures are measured at each temperature ($P/E_0=0.05$ to 0.5). For the lowest temperature, $\beta E_0=8$, extra data sets are run for $N=64$ and 192 in order to investigate finite-size effects.

At fixed temperature, the fraction of flat disks present in the sample should decrease as the pressure is raised. For high temperatures, the change from flat to upright orientation should be a smooth function of pressure, while at low temperatures the change may be more abrupt. Shown in Fig. 3 are samples of the configurations at the lowest temperature we investigate, $\beta E_0=8$. The sequence shows a wide pressure range, $P/E_0=0.1$ to 0.5 in steps of 0.1. The dimension of the observational frame remains constant in the figure; the decrease in the apparent size of the system is a result of the increasing pressure. One can see that at $P/E_0=0.1$, the system is comprised mainly of flat disks, reflecting the fact that the probability of flipping a disk is e^{-8}, ignoring pressure effects. As the pressure increases, there is a rapid change in the fraction of upright disks around $P/E_0=0.25$.

The area per particle is shown as a function of pressure for the $N=128$ system in Fig. 4. One can see that at the highest temperatures, the area decreases smoothly with pressure. At the lowest temperature, $\beta E_0=8$, the changes are more abrupt, as expected from the discussion of Fig. 3. Shown for comparison in the figure is the hexagonal close packing (hcp hereafter) area for flat disks ($2\sqrt{3}$ in units of R^2). The rapid change in area at low temperature around the hcp area may indicate that the system is nearing the critical point of a flat-to-upright phase transition.

To investigate this possibility further, shown in Fig. 5 is the fraction of upright disks

$$f\equiv\langle N_{\text{upright}}/N_{\text{total}}\rangle\ . \tag{11}$$

This quantity is proportional to the expectation of the internal energy per particle $\langle\varepsilon\rangle$:

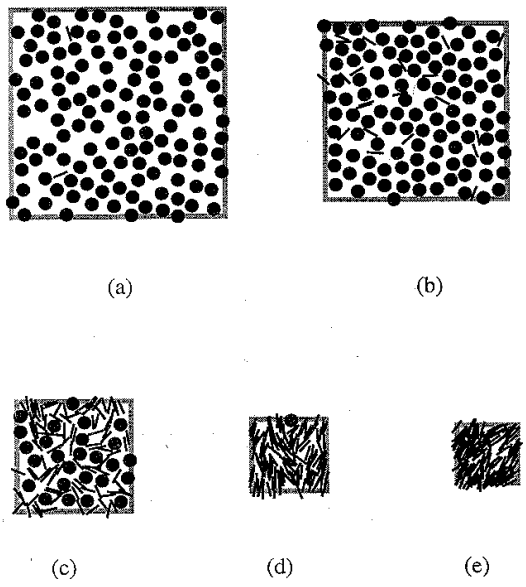

FIG. 3. Sample configurations of a 128-platelet system in the restricted orientation model ($z=0$; $\alpha=0$ or $\pi/2$). The temperature is fixed at $\beta E_0=8$, while the pressure ranges from $P/E_0=0.1$ (a) to 0.5 (e) in steps of 0.1.

$$\langle \varepsilon \rangle \equiv \langle E \rangle / N = f E_0 \ . \tag{12}$$

From the figure, one can see that the increase in f with pressure is more dramatic as the temperature decreases, although it is not discontinuous. Further, all curves pass through $f=0.58$ at around $P/E_0=0.28$. This value for P/E_0 is close to what one expects at zero temperature. Equating the energy E_0 required to flip one of the disks with $P\Delta A$, where ΔA is the area change of the system, then for hexagonally close-packed disks, $P/E_0 = 1/(2\sqrt{3})=0.29$ in units of R^2.

For there to be a first-order phase transition present at $\beta E_0=8$, then the rounding in f observed in Fig. 5 would have to be associated with finite-size effects. For this temperature only, runs are also performed on systems with $N=64$ and 192 disks and periodic boundary conditions. The results of these runs are shown in Fig. 6 for the fraction f of Fig. 5. The values of f in the figure are almost superimposable, even though N changes by a factor of 3.

Another characteristic of the system is the enthalpy per particle $H/N=(E+PA)/N$. One might expect the enthalpy to be a smoother function of P/E_0 than is f, since the increase in internal energy (proportional to f) is offset by the PA work done on the system. Rather than show the enthalpy as a function of P/E_0, in Fig. 7 we show H/NE_0 as a function of temperature k_BT/E_0 with the pressure P/E_0 fixed. Although there are not a large number of data points at any given pressure, the enthalpy does not show any abrupt changes in the figure. Again, this does not support the hypothesis of a phase transition.

Two quantities commonly used in phase-transition studies are the isothermal compressibility χ_T, defined by

$$\chi_T \equiv -\frac{1}{A}\frac{\partial A}{\partial P}\bigg|_T \ , \tag{13}$$

and the specific heat at constant pressure C_P,

$$C_P \equiv \frac{1}{N}\frac{\partial H}{\partial T}\bigg|_P \ . \tag{14}$$

One can use the fluctuations in A and H, respectively, to obtain these quantities via

$$\chi_T = \frac{\beta}{A}(\langle A^2 \rangle - \langle A \rangle^2) \tag{15}$$

and

$$C_P/k_B = \frac{1}{N}\beta^2(\langle H^2 \rangle - \langle H \rangle^2) \ . \tag{16}$$

However, the sample size available in this simulation

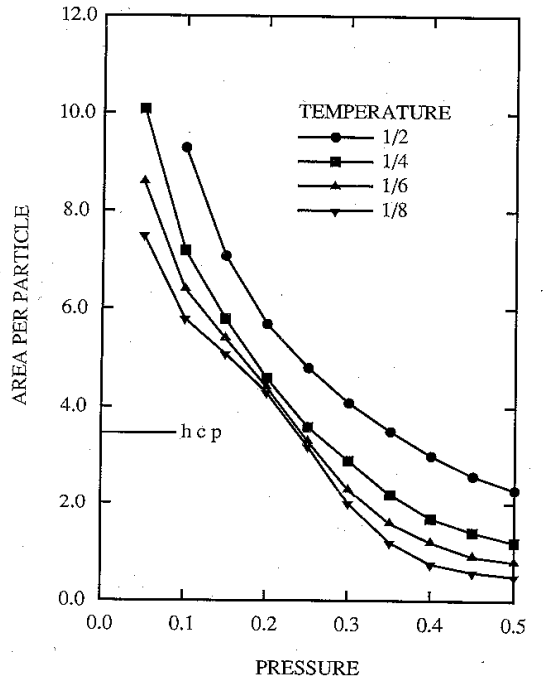

FIG. 4. Equation of state for the restricted orientation model. The area per disk (in units of R^2) is shown as a function of pressure (P/E_0) at fixed temperature for the four temperatures investigated, $k_BT/E_0=1/2$, 1/4, 1/6, and 1/8. The sample size is $N=128$ with periodic boundary conditions. The area per particle at hexagonal close packing (hcp) is shown for comparison.

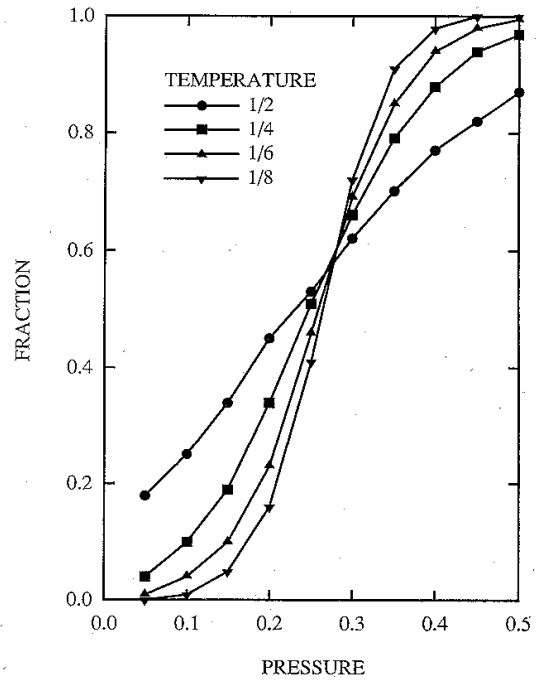

FIG. 5. Upright disks as a fraction of the total number of disks for four temperatures, $k_BT/E_0=1/2$, 1/4, 1/6, and 1/8 in the restricted orientation model. This quantity is also equal to the normalized internal energy per disk $\langle E \rangle / NE_0$. The fraction is shown as a function of pressure P/E_0.

yields less accurate values for χ_T and C_P from Eqs. (15) and (16) than can be obtained from approximate numerical differentiation of Figs. 4 and 7. We find that for neither χ_T nor C_P is there any particular evidence for discontinuous behavior or a systematic change with N. To within our limited statistics, we conclude that there is no flat-to-upright phase transition for temperatures above $k_BT/E_0=1/8$.

This is not to say that the platelets behave like a two-dimensional ideal gas, however. Particularly around $P/E_0=0.29$ there are large excursions from ideality at low temperature. This is illustrated in Fig. 8, where $\beta P\langle A\rangle/N$ is plotted against density $N/\langle A\rangle$ at fixed temperature k_BT/E_0. The ideal-gas value of $\beta P\langle A\rangle/N$ is unity, and one can see that the system tends to this value in the dilute limit $N/\langle A\rangle\to 0$ or at high temperatures $\beta E_0\to 0$. However, away from these limits there is significant nonideality, particularly near $P/E_0=0.3$. This implies that there is a substantial surface pressure required to convert from the flat-to-upright phases at low temperature.

Finally, we wish to examine the appearance of nematiclike order in the high-pressure samples shown in Fig. 3. As a measure of the orientational order in our system, we construct the expectation of the angle ϕ_i which the plane of the ith upright disk makes with respect to the x axis. We evaluate the dispersion $\Delta\phi^2=\langle(\phi_i-\langle\phi\rangle)^2\rangle_i$ of the angle for each configuration, then take the expectation $\langle\Delta\phi^2\rangle$ over all 50 configurations in each βE_0 and βP

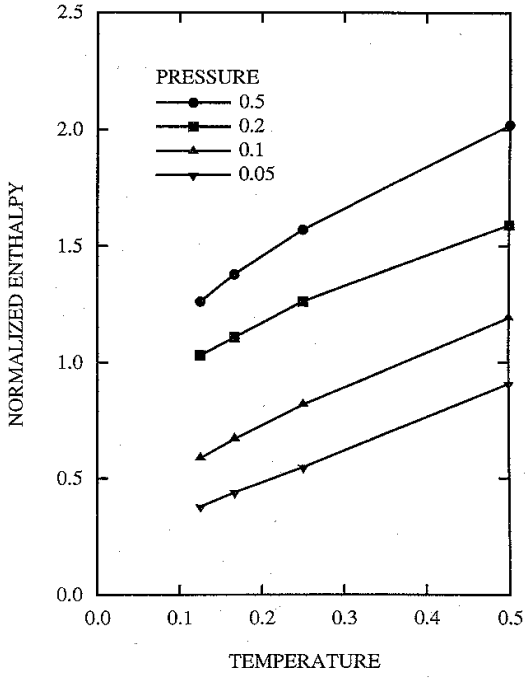

FIG. 7. Normalized enthalpy per particle H/NE_0 in the restricted orientation model shown as a function of temperature k_BT/E_0 at fixed pressure P/E_0. The data are obtained for $N=128$.

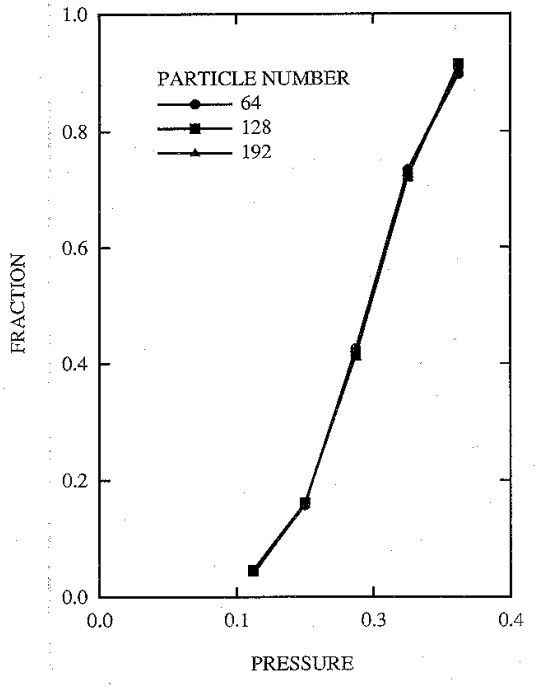

FIG. 6. System-size dependence of the upright disk fraction as a function of pressure P/E_0 as in Fig. 5. Data for $N=64$, 128, and 192 are shown at $\beta E_0=8$. The curves are virtually superimposable.

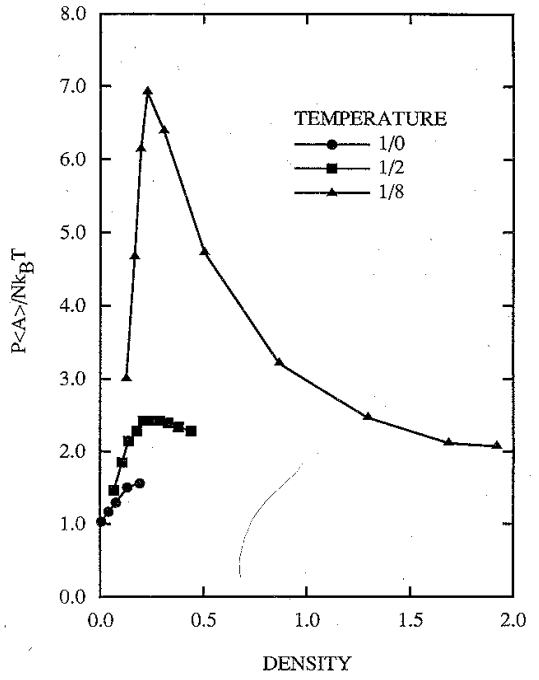

FIG. 8. Deviation from ideal-gas behavior in the restricted orientation model. The quantity $\beta P\langle A\rangle/N$ is shown as a function of density $N/\langle A\rangle$ for fixed temperature ($k_BT/E_0=1/0$, 1/2, 1/8).

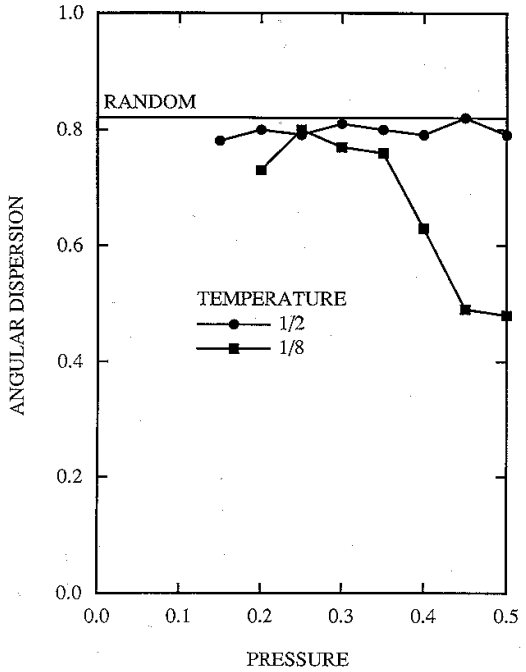

FIG. 9. Average dispersion of the orientation angle $\langle \Delta\phi^2 \rangle$ in the restricted orientation model as a function of pressure P/E_0 at fixed temperature ($k_BT/E_0=1/2$ and $1/8$). For each of 50 configurations at a given temperature and pressure, values of $\langle \phi \rangle$ and $\Delta\phi^2$ are constructed. Then an average is performed over all 50 configurations to obtain $\langle \Delta\phi^2 \rangle$. The value of $\langle \Delta\phi^2 \rangle$ for purely random orientations is shown for comparison.

sample. The results of this calculation are shown in Fig. 9 for two temperatures, $k_BT/E_0=1/2$ and $k_BT/E_0=1/8$.

At $k_BT/E_0=1/2$, there is no deviation from the random orientation value of $\langle \Delta\phi^2 \rangle=\pi^2/12$ over the range of P/E_0 investigated. However, at low temperatures, $\langle \Delta\phi^2 \rangle$ decreases rapidly above $P/E_0=0.4$. This decrease is clearly not associated with the flat-to-upright transition observed at P/E_0 near 0.28, and is associated with the onset of nematic ordering. Since this ordering has been extensively investigated elsewhere[8–11] for hard ellipsoids and spherocylinders, we do not examine it further here.

VI. CONCLUSION

We investigate the properties of a model for amphiphilic platelets at an interface between immiscible liquids. The platelet is modeled as a hard cylinder whose faces and edge are differentially attracted to the two liquids. The ground states of the model have the platelet residing at the interface in a flat or upright position over almost all of the model's parameter space; in no situation is it energetically more favorable for a platelet to be completely surrounded by only one of the liquids. This behavior is similar to what is observed experimentally.

For some range of parameters, the upright position is metastable with respect to the flat orientation. Even though it may be energetically less favored, the upright position may be entropically favored, depending on cylinder geometry. Hence, there may be a rapid change from flat-to-upright orientation as a function of pressure at fixed temperature. To investigate this possibility, we develop a restricted orientation model in which the center of the platelet is made to lie at the interface and the orientation is allowed to be either flat or upright. In this model, the fraction of upright platelets smoothly increases with pressure at high temperature. The change is more abrupt at low temperature. However, at the lowest temperature investigated, finite-size effects do not show behavior expected for a flat-to-upright phase transition, nor do the isothermal compressibility or the specific heat at constant pressure.

The pressure at which the orientation change occurs is consistent with a simple argument which equates the energy cost in changing the platelet's orientation with the $P\Delta A$ work done. Around this pressure, the behavior of the platelet system is far from a two-dimensional ideal gas and there is a significant surface pressure. This pressure may be a small contributor to the experimental observation[4,5] that a film of platelets may rise up the side of a vessel containing the liquids forming the interface. At the highest pressures, the platelets in the restricted orientation model appear to form a nematic phase, although we have not investigated the characteristics of this phase with any thoroughness.

How the behavior shown in the restricted orientation model is modified in the full model is currently under investigation, although the calculation is very compute intensive. Further work will entail the addition of an interplatelet attractive potential to more realistically model interfaces with high platelet density.

ACKNOWLEDGMENTS

The authors wish to thank M. Plischke, B. Bergersen, and R. Frindt for many stimulating discussions. This work is supported in part by the Natural Sciences and Engineering Research Council of Canada.

APPENDIX

In principle, the Hamiltonian for the platelet-interface interaction involves the calculation of five areas: the areas of the platelet faces exposed to liquids 1 and 2 (A_{F1} and A_{F2}), the areas of the platelet edge exposed to the liquids (A_{E1} and A_{E2}), and the liquid interfacial area that the platelet displaces (A_{12}). In practice, we need consider only three areas, the remainder being determined through the trivial relationships

$$A_{F1}+A_{F2}=2\pi R^2 \tag{A1a}$$

and

$$A_{E1}+A_{E2}=2\pi RT\ . \tag{A1b}$$

We reproduce the analytical expressions for the areas, considering only the ranges $z\geq 0$ and $0\leq\alpha\leq\pi/2$. Ex-

pressions for $z \leq 0$ can be obtained from these using Eq. (A1) and symmetry arguments.

Case I. No intersections with platelet faces

$$A_{F2}=\pi R^2 , \tag{A2a}$$

$$A_{E2}=2\pi R\left[\frac{T}{2}-\frac{z}{\cos\alpha}\right] , \tag{A2b}$$

$$A_{12}=\pi R^2/\cos\alpha . \tag{A2c}$$

Case II. Intersection with one platelet face

$$A_{F2}=R^2(\theta-\sin\theta\cos\theta) , \tag{A3a}$$

$$A_{E2}=2R^2\tan\alpha(\sin\theta-\theta\cos\theta) , \tag{A3b}$$

$$A_{12}=R^2(\theta-\sin\theta\cos\theta)/\cos\alpha , \tag{A3c}$$

where

$$\cos\theta=\left[\frac{z}{R}-\frac{T}{2R}\cos\alpha\right]\Big/\sin\alpha , \quad 0\leq\theta\leq\pi . \tag{A4}$$

Case III. Intersection with both faces

$$A_{F2}=R^2(\theta_L-\sin\theta_L\cos\theta_L+\theta_U-\sin\theta_U\cos\theta_U) , \tag{A5a}$$

$$A_{E2}=2R^2\tan\alpha(\sin\theta_L-\theta_L\cos\theta_L-\sin\theta_U+\theta_U\cos\theta_U) , \tag{A5b}$$

$$A_{12}=R^2(\theta_L-\sin\theta_L\cos\theta_L-\theta_U+\sin\theta_U\cos\theta_U)/\cos\alpha , \tag{A5c}$$

where

$$\cos\theta_L=\left[\frac{z}{R}-\frac{T}{2R}\cos\alpha\right]\Big/\sin\alpha , \quad 0\leq\theta_L\leq\pi \tag{A6a}$$

$$\cos\theta_U=\left[\frac{z}{R}+\frac{T}{2R}\cos\alpha\right]\Big/\sin\alpha , \quad 0\leq\theta_U\leq\pi . \tag{A6b}$$

*Present address: Department of Chemistry, University of Toronto, Toronto, Ontario, Canada M5S 1A1.

[1]D. W. Murphy and G. W. Hull, J. Chem. Phys. **62**, 973 (1975).
[2]C. Liu, O. Singh, P. Joensen, A. E. Curzon, and R. F. Frindt, Thin Solid Films **113**, 165 (1984).
[3]P. Joensen, R. F. Frindt, and S. R. Morrison, Mater. Res. Bull. **21**, 457 (1986).
[4]W. M. R. Divigalpitiya, R. F. Frindt, and S. R. Morrison, Science **246**, 369 (1989).
[5]W. M. R. Divigalpitiya, S. R. Morrison, and R. F. Frindt, Thin Solid Films **186**, 177 (1990).
[6]B. K. Miremadi, T. Cowan, and S. R. Morrison, J. Appl. Phys. (to be published).
[7]T. Garel, D. A. Huse, S. Leibler, and H. Orland, Europhys. Lett. **8**, 9 (1989).
[8]L. Onsager, Ann. N.Y. Acad. Sci. **51**, 627 (1949).
[9]A. Poniewierski and R. Holyst, Phys. Rev. Lett. **61**, 2461 (1988).
[10]D. Frenkel and B. M. Mulder, Mol. Phys. **55**, 1171 (1985).
[11]J. A. C. Veerman and D. Frenkel, Phys. Rev. A **41**, 3237 (1990) and references therein.
[12]See, for example, M. J. P. Gringas, P. C. W. Holdsworth, and B. Bergersen, Europhys. Lett. **9**, 539 (1989).
[13]For a summary of Monte Carlo techniques in liquid studies, see J. P. Hansen and I. R. McDonald, *Theory of Simple Liquids* (Oxford University Press, New York, 1986). Computational techniques for isobaric systems can be found in W. W. Wood, J. Chem. Phys. **48**, 415 (1968).